

# **Relationships between Breakthrough Curves and X-ray Computed Tomography Analyzed Macropore Characteristics**

Ten undisturbed soil monoliths of clayey Pelosol at Gottingen, Germany covering the horizons A<sub>1</sub> and P were collected. Some columns were left at natural humidity, some were oven-dried to simulate drought situations in forest soils in consequence of climate change. In seven columns, four micro-lysimeters, each, were installed at half height in order to obtain data for analysis of single solute pathways. A fixed amount of KBr tracer was applied to the humus layer. The columns were irrigated with CaCl<sub>2</sub>. Column output and lysimeter output were collected and analyzed to record breakthrough curves. Bimodal analytical convection dispersion equation (CDE) solutions were fitted for the column outputs using a non-linear least squares fit. A simple CDE solution did not fit well. This supports the model of two overlaying transport phenomena. After breakthrough recording was complete, all columns were scanned using X-ray computed tomography (CT). From the CT data 3-D reconstructions of the porous system were created for visual inspection, and the exact pathways for macropores along the micro-lysimeters were determined. Additionally, indices of the pore structure were computed to compare with the slow and fast dispersivity values from the bimodal CDE fit. The variation in micro-lysimeter performance could be explained using the 3-D reconstruction. Statistically significant differences between the pore structure of wet and dried columns after the end of irrigation could not be identified. The pore index has generally a negative linear relationship with the fast dispersivity, and a positive linear relationship with the slow dispersivity. These relations are stronger in topsoil. The CT pictures and 3-D reconstructions provide an interesting insight into the soil pores system and may help to understand man-made drought problems due to climate change.

**Keywords:** Tracer transport, X-ray computed tomography, 3-D visualization, bimodality, CDE, dispersivity, BTC/breakthrough curves

The main research question of this work was to find out, if single pathways in unsaturated flow of wet and dried soils (with regard to droughts due to climate change) could be characterized in their functions. Quantitative relationships between soil structure (especially macropore characteristics, namely their size, number, type, distribution and continuity) and soil hydraulic properties are essential for improving our ability to model flow and transport in structured soils. Bouma (1979) and others have used chloride breakthrough curves from undisturbed soil columns

as an indirect means of characterizing macropores. In recent years, X-ray computed tomography (CT) data, which is based on varied linear attenuation of water, air and solid materials, provided an attractive tool for soil scientists to non-invasively observe soil structure (Gantzer and Anderson 2002; Luo et al. 2008; Taina et al. 2008; Kumare et al. 2010). Warner et al. (1989) used CT data to investigate the macropore system, e.g. characterization of cracks, earthworm holes and rooting channels. Peyton et al. (1992) concentrated on macropores, quantifying macropore perimeters, the paths surrounding macropore shapes. A relationship between macropores visualized by CT data and preferential flow was investigated by Heijmans et al. (1996). Luo et al. (2010) related macropore characteristics quantitatively to solute transport parameters under saturated conditions. Borges and Pires (2012) have studied the representative

**Table1.**Descriptionofexperimentaldesign

Columnnumber	Treatment (type)	watercontent(%) (mean)	Br-Pulse $t_0$ [day] (Bramount[mg])	Recoveryrate(%)
1-4	Naturalhumidity (1)	37.5	0.833 (14.9-16.4)	76.9-85.9
5-7	Oven-dried (2)	30.7	0.833 (15.8-18.3)	55.2-91.1
10-12	Oven-dried (3)	30.7	0.0833 (15.3-17.3)	46.6-68.0

elementaryarea(REA) ofsoilsamplesusingCTdata, andconcludedthatsampleswithvolumesfrom50 cm<sup>3</sup>to100cm<sup>3</sup>withminimumcrosssectionof640 mm<sup>2</sup>areenoughtoberepresentativeforthesoil structure.Oursoilssampleshadvolumesofabout5000 cm<sup>3</sup>withacrosssectionof169cm<sup>2</sup>.

ThepresentstudywascarriedoutatUniversity ofGöttingen,InstituteforSoilScienceandForest Nutrition,Büsgenweg,GermanyonsoilcolumnsofaclayeyPelosol(VerticCambisol)withwelldescribedswell-shrinkcharacteristics(Spangenbergetal.2011).Theobjectivesweretostudytheroleofporecontactofmicro-lysimetersinthesoilcolumnnontracertransportinrelationtothestructure,assessedbyX-rayCTunderdifferentinitialconditionsand irrigation.Asitisnotpossibletocarryoutthese investigationsunderfieldconditions,non-destructive CTdatawereused,makingitpossiblefor3-Dreconstructionofthestructureoftheinvestigatedsoil columns.Furthermore,usingCTdata,anattemptwas madetounderstandtherelationshipbetweenthe breakthroughcurvesofthetracers(velocity, dispersionanddispersivity)andthemeasuredvolume andstructureofthepores.

## MaterialsandMethods

### Theoilstudied

Theoilinthe presentstudyisaclayeyPelosol(Vertic Cambisol),developedfromaMuschelkalk(shell-lime)plateauderivedfromTriassic sediment layers.CollectedhorizonswereO<sub>lf</sub>-A<sub>h</sub>-P,O<sub>lf</sub>wasremoved,onlyA<sub>h</sub>-Premained.ThePhorizon showedapolyedricstructure(loamyclay).Inthis horizon,swell-shrinkcharacteristicsarewell expressed,andswellingclaymineralsaccountedfor26±5 %.Mineralcompositionsshowquartz,illite, corrensite,orthoclase,albiteandgoethite.Thedetails ofthesoilsandtheexperimentalsetupweregivenin Spangenbergetal.(2011).Arepresentativesample wastakenintheareawherethesoilcolumnswere

taken.Thissamplewasanalyzedforsoildensityin variousdepths.Bulkdensityrangedfrom0.908Mg m<sup>-3</sup>(topsoil,A<sub>h</sub>)to1.569Mgm<sup>-3</sup>(subsoil,P,20-30 cmdepth).

### Thecolumnexperiment

Originally,twelveundisturbedsoilcolumnswere collectedinplexiglasscylindersof14.7cm diameterandabout30cmheightfroma4m<sup>2</sup>sampling area.Tencolumnswereselectedforthistudy,butin ordertoreducethetotalamountoffiguresonly columns1,5and12arepresentedanddescribedindetail.Table1showsanovaiewoftheexperimental design.Fourcolumns(1-4)werekeptattheirnatural meanwatercontentofabout37.5%(meanvalue, n=4).Columns5-7and10-12weredriedat105°Cin aheatingcabinettoawatercontentof30.7%(Table1).Four micro-lysimeters,each,wereinstalledin sevensoilcolumns.Thesemicro-lysimeterswere equippedwithahydrophilicporouspolymertube (diameter2.3mm),madebyEijkelkampAgrisearchEquipment,Netherlands(Spangenbergetal.1997). Theyweredesignedspecificallytomiminizethe impactofinstallationintosoil.Theywereinstalledat abouthalftheheightofthecolumninordertoallowobservati onoftheflowparametersinhightemporal andspatialresolutioninadditiontothebottomoutput. Allcolumnswereirrigatedinavacuumpacked plexiglascontainer,whichisacompleteoil microcosm(describedinSpangenbergetal.2011). Irrigationwasappliedusinganelectronicdeviceevery 2h.Atthebottomofeachmonolith,unsaturatedflowwasadjustedto300hPa.Abromidepulsewasapplied toeachcolumnatthebeginningoftheexperiment. ThenregularirrigationwithCaCl<sub>2</sub>wasstarted,which lastedforatleast30days,*i.e.*untilnomorebromide wasfoundinthecolumnoutput.Solutionsampleswerecollecteddailyatthebottomandfromthemicro-lysimetersofeachcolumn.Theywereanalyzedfor chlorideandbromide.AnalysesweredonebyHPLC ionchromatography.Elutionmixturecontained

$\text{Na}_2\text{CO}_3$  (2 mmol) and  $\text{NaHCO}_3$  (0.75 mmol). Detection limit of both elements was  $300 \mu\text{g L}^{-1}$ . The statistical analysis was done using SAS (Statistical Analysis System, SAS Institute, Inc., Cary). The procedure “nlin” of SAS was used to provide least squares modeling. An analytical solution of the convection dispersion equation (CDE) was used to fit the breakthrough curves of the experiment (van Genuchten 1982). Model parameters were estimated using bimodality, since it resulted in the best fit (Spangenbergetal. 2011).

### BTC Modeling

The most important model for solution transport in soil describes concentration changes in time and space using the CDE according to Nielsen and Biggar (1962).

$$R \frac{\partial C}{\partial t} = D \frac{\partial^2 C}{\partial x^2} - v \frac{\partial C}{\partial x} \quad \dots(1)$$

where,  $C$ =concentration [ $\text{ML}^{-3}$ ];  $t$ =time [days];  $x$ =spatial distance [L];  $D$ =dispersion coefficient;  $v$ =average pore velocity [ $\text{LT}^{-1}$ ]

$$R=\text{Retardation (dimensionless)} \quad R=1+\frac{\rho_b K_d}{\theta} \quad \dots(2)$$

where,

$\rho_b$ =soil density [ $\text{ML}^{-3}$ ];  $K_d$ =constant factor [ $\text{L}^3\text{M}^{-1}$ ];  $\rho$ =volumetric water content [ $\text{L}^3\text{L}^{-3}$ ]

According to Toride et al. (1995)  $R$  can be set on 1.

Starting (1.0) and boundary conditions (1.1 and 1.2) are:

$$C(x,0)=C_i \quad \dots(1.0)$$

$$\left(-D \frac{\partial C}{\partial x} + v\right)|_{x=0} = \begin{cases} vC_0 & 0 < t \leq t_0 \\ 0 & t > t_0 \end{cases} \quad \dots(1.1)$$

$$\frac{\partial C}{\partial x}(\infty, t)=0 \quad \dots(1.2)$$

Assuming altered infiltration and disturbed water flow due to soil drought the conditions for application of the CDE on treatment type 2 and 3 (Table 1) were incomplete. But concentrating on the aim of the investigation—a comparison between different experimental variants of dried and humid soils—the same methods of data analysis had to be chosen. To consider different flow behavior of dried and non-dried soils some new boundary conditions for the use of an analytical solution of the CDE were involved (Nielsen and Biggar 1962). A bimodal variant of this CDE was used, more details on this part are provided in Spangenbergetal. (2011).

### X-ray computed tomography

After the irrigation phase, the columns with installed micro-lysimeters were tomographed in Hospital of Goettingen University. A medical CT scanner (HiSpeed Advantage, General Electric) was used. For the purpose of four 30 cm long soil columns, the head-neck settings were chosen. To understand the differences between moist and dry treatments, each soil column was tomographed individually. The output of the CT unit is in Hounsfield Units (HU), which is an internationally standardized numbering scale (Petrovic et al. 1982). The numerical value of Hounsfield Unit depends on the attenuation coefficient of the subject matter relative to that of water (Hainsworth 1983; Grever et al. 1989; Heijset al. 1995), which is given as  $H=1000(\mu-\mu_w)/(\mu_w-\mu_a)$ . Here,  $\mu$  is the linear attenuation coefficient of the material or pixel in question,  $\mu_w$  and  $\mu_a$  are the attenuation coefficients of water and air, respectively. A 512 by 512 matrix of pixel data was obtained for each scan. A pixel had the width of about 0.76 mm. The scan was taken at intervals of 2 mm (ca 140 scans per column). A constant 1000 was added to every value, which is used on all CT scanners, and given in formula for  $H$ . After this addition, air has a value of 0 and water 1000. For each pixel, the X-ray attenuation values were restored as values from 0 to 4095. This range was due to the 12-bit processing of the tomography equipment. The high values correspond to the metal of the micro-lysimeter. The PV-WAVE was used for computer analysis, which allowed reconstructing, visualizing and quantifying 3-D macropore structure in the soil column (Pierret et al. 2002).

### Indicators for pore structure

The most important outcome of the CT data is the information on the content of solids and soil porosity. The 12-bit data was reduced to 8-bit data and the whole dataset was scaled by dividing all the values by a factor 16, so that we have values ranging from 0–255. Good spatial resolution can be achieved when there is a large difference in  $H$  values between a subject (e.g. a soil pore) and the background (e.g. soil matrix) as suggested by Grever et al. (1989).

In the present study, the same interior region of the top-and subsoil in all the soil columns was selected, the area around the micro-lysimeters was intentionally left out. The selected interior regions were divided into roughly cubic areas. These cubes form the basis for further data processing. Ideal cubes

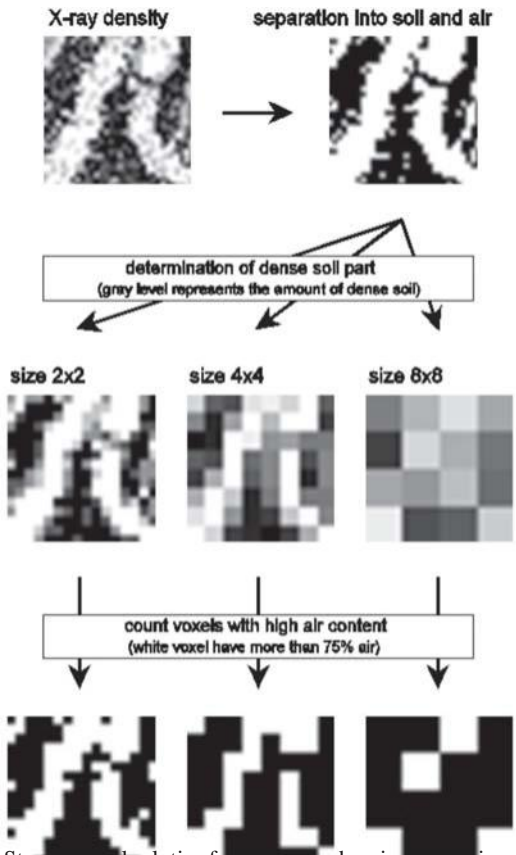


**Fig.1.** Step wise calculation for the three cube-sizes. (distribution of X-ray attenuation values à separation of soil solids and air; determination of soil solids – (gray areas show the extent of soil solids); cube size 2×2 cube size 4×4 cube size 8×8 counting of cubes with high air volumes (white cubes have more than 75% air volume))

are not possible with the given voxel size. Therefore, different sizes were considered, namely, [4,4,1] voxel (labeled 2×2), [8,8,2] voxel (labeled 4×4) and [16,16,4] voxel (labeled 8×8). These cubes correspond to volumes from 18 mm<sup>3</sup> to about 1 cm<sup>3</sup>. The step-wise calculation for the 3 cubes is presented in figure 1.

First a threshold was selected to distinguish between dense matter and pores. A value of 110 was selected, as this provided the best separation based on known material allocations. The percentage of cubes with less than 25% dense soil was computed for each sample area and cube size, which are labeled P<sub>1</sub>, P<sub>2</sub> and P<sub>4</sub>, depending on cube size. These were used as indexes for the pore structure of a column. For a completely homogeneous material, all indexes would be the same. We used P<sub>1</sub> as an index for the fine pore structure and P<sub>4</sub> is an index for the coarse pore structure. The indexes do not represent the connectivity of porous volume, only the amount of

pores at a specific scale. The dispersivity values from bimodal tracer description were related to these indices of pore structure at three different scales. These indices were compared to the dispersivity results of the CDE models.

### 3-D reconstruction of soil structure

In the core of the column, which has a cross-sectional area of about 10 cm×10 cm, the voxels with scaled attenuation values from 0 to 30 were reconstructed as a 3-D image of soil structure. This allows a visual inspection of pore connectivity for qualitative analysis. A value of 30 was chosen to allow the air-filled inner parts of macropores to be visible. For a better view of the pore contact of each lysimeter, the slice with the lysimeters was reconstructed separately in three viewing angles (40°, 70° and 85°) with same viewing angle in all cases, i.e. for all columns (Figs. 2, 3 and 4). However, only a slice with 40 degrees viewing angle was presented. In order to overcome the effect of air pockets in the outer space around the soil column, the central square area of 10 cm×10 cm was selected for the 3-dimensional reconstruction. At the top a well was at the bottom some slices of the column were discarded. The location of the micro-lysimeters in the column were established, in which the x-, y- and z-coordinates of the lysimeter head and terminal in the cross-section image were determined.

## Results and Discussion

### Influence of placement of micro-lysimeters and their function

The suction lysimeters of the tracer experiment drain different quantities of solution, although during the entire conduct of the experiment, a suction of 0.030 MPa was maintained. The great variability in the quantity of drained solution appears to be caused by the difference in positioning of the micro-lysimeters in the columns, relative to the porous system of the column. Preferential flow may initially have bypassed the lysimeters altogether, but relative position to the porous system seems to have a high influence. In order to explain this phenomenon, one column in each group is presented in figures 5, 6 and 7. Each figure contains a cross section image at the height of the micro-lysimeters, as schematic of micro-lysimeter placement and the daily amounts of solution drained. The figures are used to judge the relative performance of the lysimeters. All four lysimeters of column 1 show similar performance (Fig.

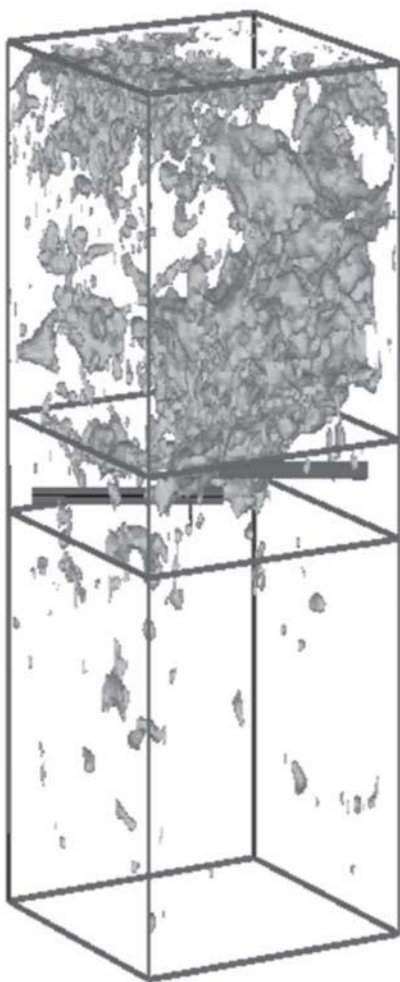


Fig.2a,Column1,withsection

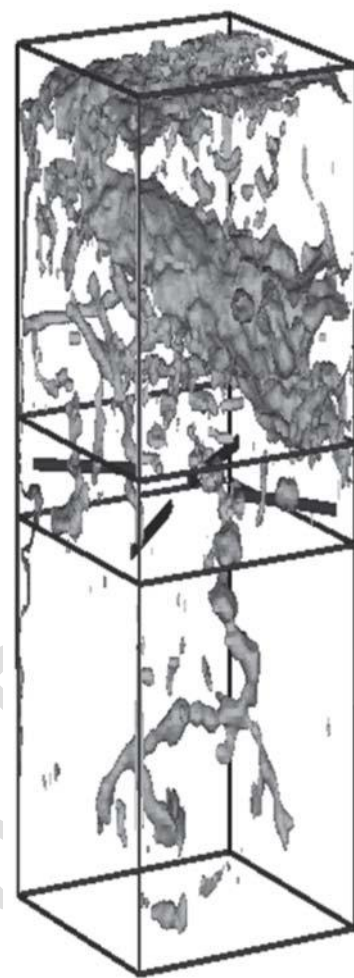


Fig.3a,Column5,withsection

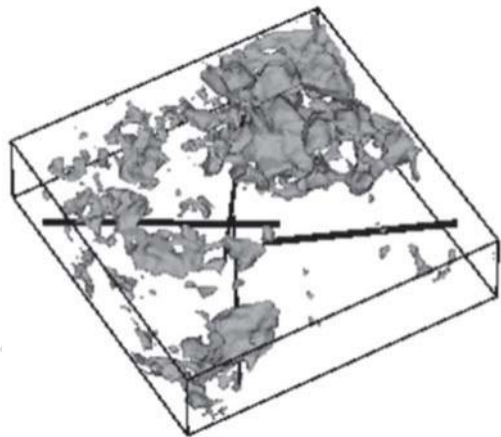


Fig.2b,Column1,section,40degree

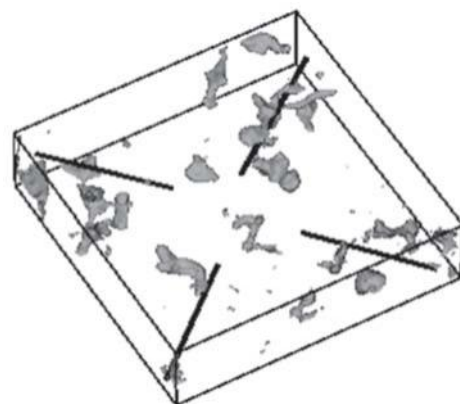


Fig.3b,Column5,section,40degree

**Fig.2.3**-Dreconstructionofcolumn1(experimentalvariant 1)withinstalledmicro-lysimeters.Inthecoreofthe column,thescaledattenuationvaluesfrom0to30are presented.Forabetterview,thesectionwiththelysimetersispresentedina40degreelook-angle.Thecore ofthecolumnhasacross-sectionalareaof10cm×10cm

**Fig.3.3**-Dreconstructionofcolumn5(experimentalvariant 2)withinstalledmicro-lysimeters.Inthecoreofthe column,thescaledattenuationvaluesfrom0to30are presented.Forabetterview,thesectionwiththelysimetersispresentedina40degreelook-angle.Thecore ofthecolumnhasacross-sectionalareaof10cm×10cm

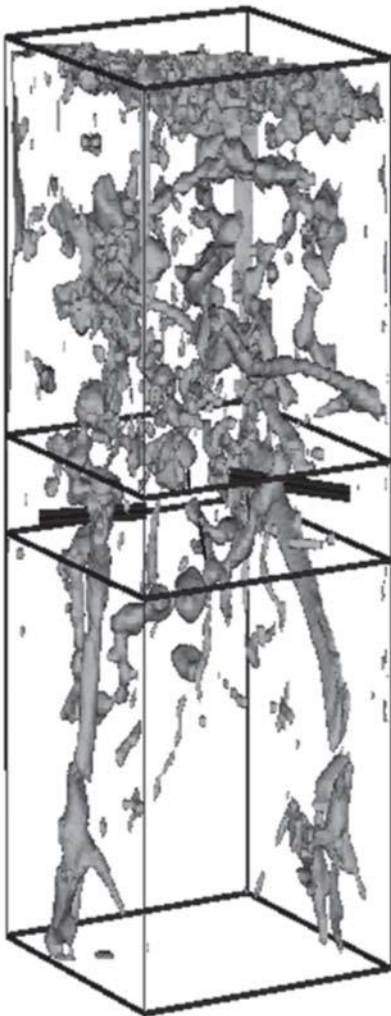


Fig.4a,Column12,withsection

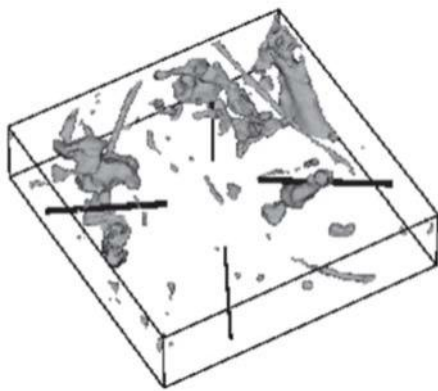


Fig.4b,Column12,section,40degree

**Fig.4.3**-Dreconstructionofcolumn12(experimentalvariant 3)withinstalledmicro-lysimeters.Inthecoreofthe columnthescaledattenuationvaluesfrom0to30are presented.Forabetterview,thesectionwiththelysimetersispresentedina40degreelook-angle.Thecore ofthecolumnhasacross-sectionalareaof10cm×10cm

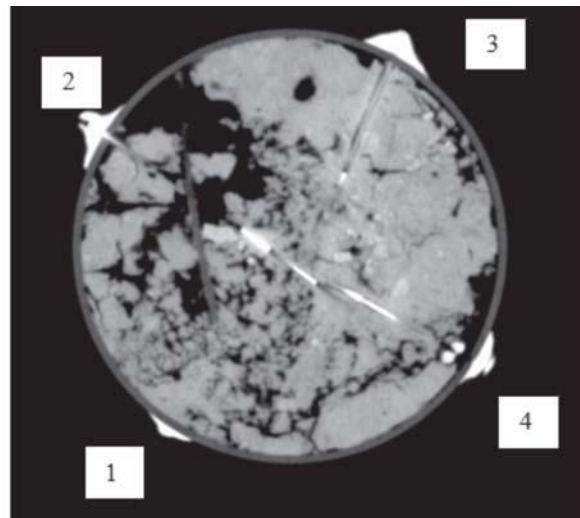


Figure5a,cross-sectionofcolumn1withmicro- lysimeters(topleft:no2;topright:no3;bottomleft:no1;bottomright: no4)andtheirnumbering

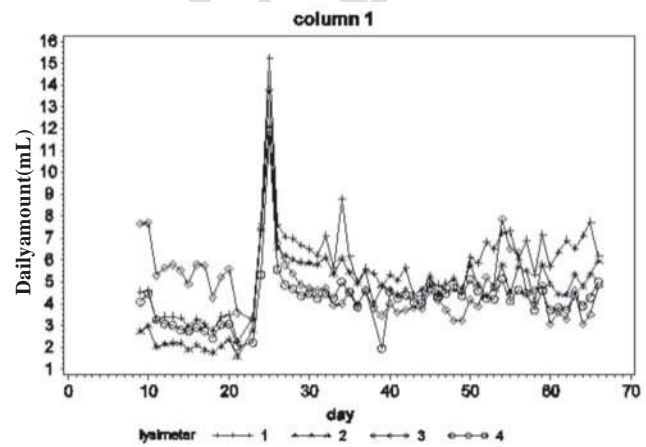


Fig.5bSamplevolumes(ml)ofcolumn1

**Fig.5.**Cross-sectionimageofcolumn1withmicro-lysimetersandtheirnumbering(5a)aswellasmicro-lysimeters'respectivemeasuredsamplevolumes(mL),column1(5b)

5c).Micro-lysimeters2and4showidenticalcurves, evenbeforeandafterthebreakincontinuityof leaching.Theirtipslieclosetoeachother(Fig.5a and5b),soweassume,thesesuctionlysimetersshowedreciprocalinfluence.Modelingofthe breakthroughcurvesdidn'tmakesense.Incolumns5 and12,bothpreviouslydried,atleastonemicro-lysimeterhaddirectcontacttoamacropore(Fig.6a, micro-lysimeterno4andFig.7amicro-lysimeterno 15).Thesemicro-lysimetersshowedthelowestsuction performancewithintheircolumn.Thus,contacttoa macropore(>0.5cm)appearstohaveaclear influenceonthesuctionperformanceofamicro-

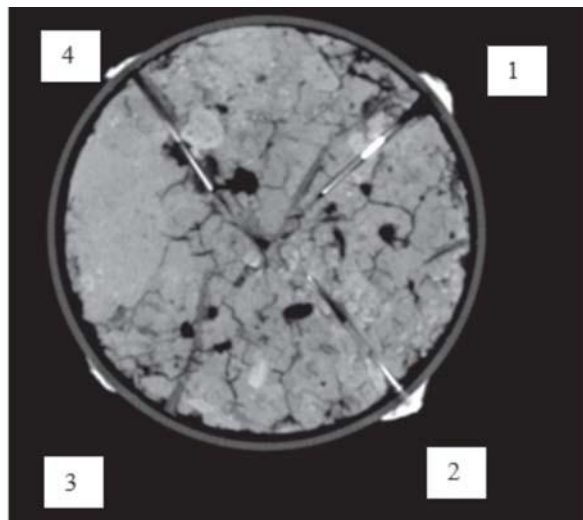


Fig.6a cross-section of column 5 with micro-lysimeters (top left: no 4; top right: no 1; bottom left: no 3; bottom right: no 2) and their numbering

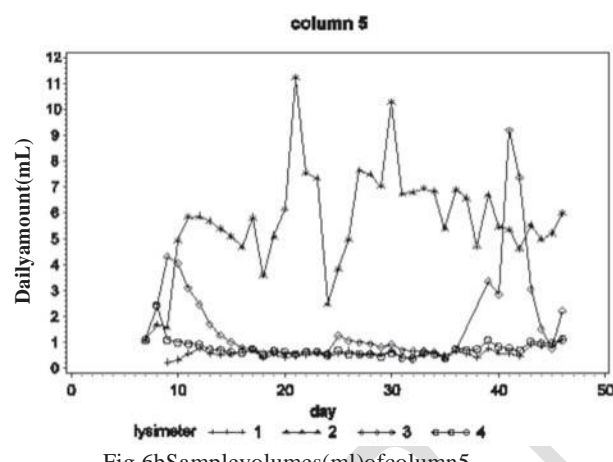


Fig.6b Sample volumes (mL) of column 5

**Fig.6.** Cross-section image of column 5 with micro-lysimeters and their numbering (6a) as well as micro-lysimeters' respective measured sample volumes (mL), column 5(6b)

lysimeter. Under unsaturated conditions, only a thin film of water is present on the walls of pores of this diameter. Because of this, the suction lysimeters drained no solution most of the time, and hence low volume of leachate. Transferring this result to natural conditions where the micro-lysimeters would represent the rooting zone of forest trees it can be assumed that already under these simulated drought conditions water stress would have begun.

Micro-lysimeters in a compact soil matrix also showed low suction performance. A placement avoiding these extremes resulted in satisfactory functioning. If enough fine pores are present in the vicinity of the micro-lysimeters, the capillary

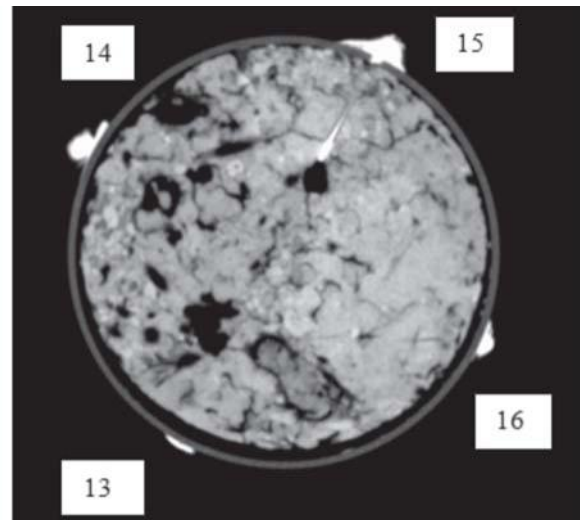


Fig.7a Cross-section of column 12 with micro-lysimeters (top left: no 14; top right: no 15; bottom left: no 13; bottom right: no 16) and their numbering

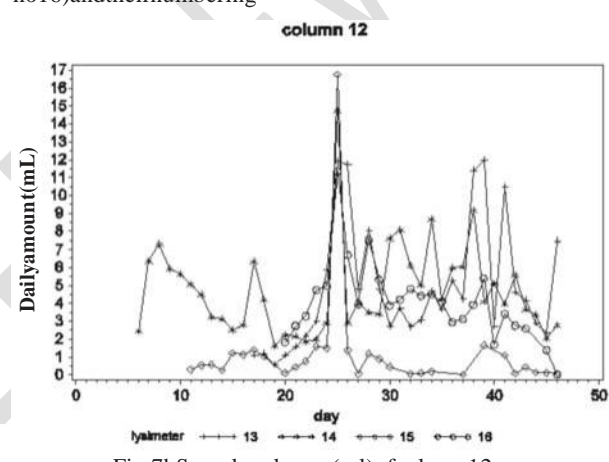
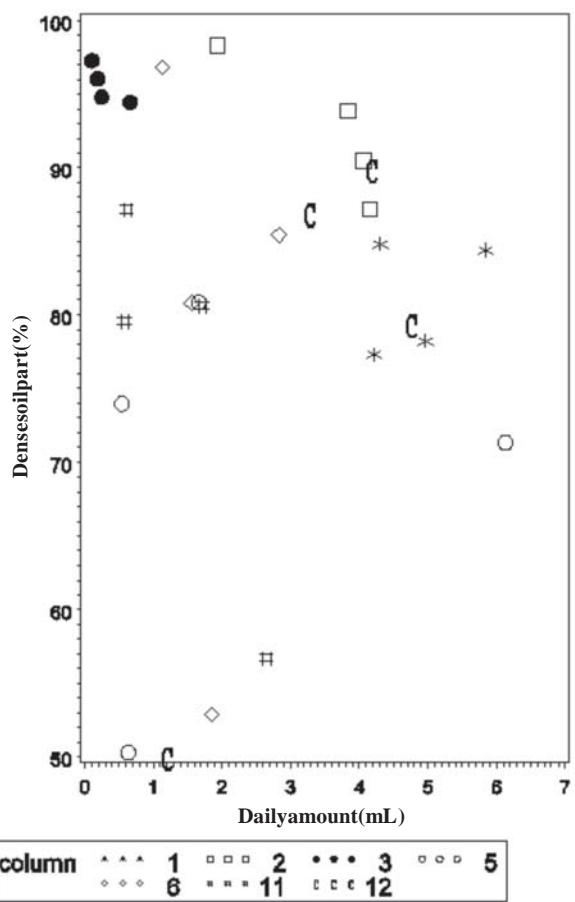


Fig.7b Sample volumes (mL) of column 12

**Fig.7.** Cross-section image of column 12 with micro-lysimeters and their numbering (7a) as well as micro-lysimeters' respective measured sample volumes (mL), column 5(7b)

contribution of water outweighs the air-filled porosity, and the volume of the leachate collected will be higher (Fig.8). The median daily amount of leachate after the initial phase of the experiment is shown on the abscissa. On the ordinate, the content of the solids in the soil in an ellipsoidal region around the tip of the micro-lysimeter ( $\text{ca. } 12 \text{ cm}^3$ ) is shown. Interestingly, the suction performance of the micro-lysimeter with high pore volume was as poor as for lysimeter with almost 100% compact soil around it (column 3). Most lysimeters show best performance with moderately compact soil. In addition to the total quantity of pores and soil volume, the pore size distribution and their connectivity to the immediate vicinity of the lysimeter



**Fig.8.** Percentagesoilssolidarounds thelysimeterinrelation tothesuctionperformanceofthelysimeterfor28lysimetersin7columns. Thesoilsolidcontentwasobtained fromtheCTattenuationdata

isimportant. Allthese factors appear to beresponsible for the otherwiseunexplained suctioneffectiveness ofthelysimeters. Eightofthe28lysimeters haveto beconsideredtobeineffective,since theydrainless than  $1\text{mLd}^{-1}$ (Fig.8). About70% oftheinstalled micro-lysimetersarecapableofdraining, andabout halfofthemaredistinctlyuseful( $>3\text{mLd}^{-1}$ ) underthegivenconditions.

For thefirsttime, CTanalysiswasabletovisualize and reveal cause-effect relationships of micro-lysimeterpore contacts and their suctionability. The X-ray CT images of cross sections of the soil columns didnot show noticeable disturbance in soil structure of thecolumnsdueto installation of the micro-lysimeters(Figs.5a,6aand7a). In contrast to this, Beckmann et al. (1992) found noticeable disturbances in soil structure due to installation of standard lysimetercups in thefield, resulting in an alteration of theporesystem. Formost of thedried

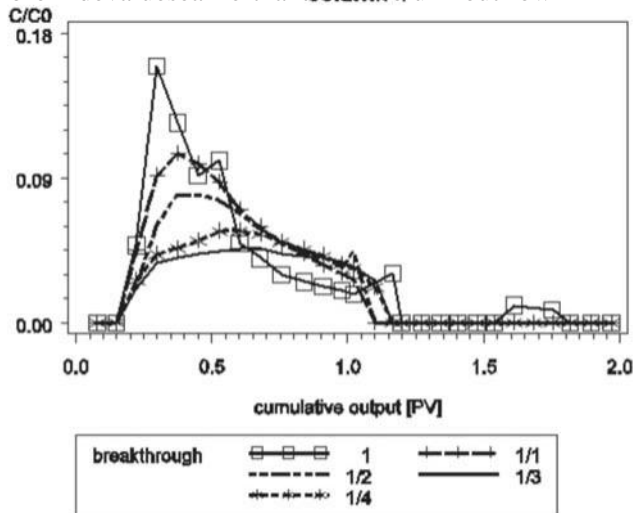
columns(columns5and12; Figs.10and11) the micro-lysimeters havemissed themainbreakthrough astheyhadnoinitialsoilcontactbecauseofthedry stateofthesoil, or the firstfastbreakthrough bypassed them.

#### *Localization of the micro-lysimeters and its relation to tracer breakthrough curves*

Given that no CDEmodel could befit for the micro-lysimeter data, its breakthrough curves in relation to porestructure canonly bediscussed in a qualitative way. As examplesthe 3-Dreconstructions of columns 1, 5 and 12 with installed micro-

lysimeters arepresentedin figures 2, 3 and 4, respectively.

The breakthrough curves of all micro-lysimeters areavailable aswell as all 3-Dreconstructions of the scannedsoilcolumns. The breakthroughs of the micro-lysimeters of column 1 (thewetvariant of the experiment) alongwith thebreakthrough of the whole column arerepresented (Fig.9). In thiscolumn, the maximum values of the micro-lysimeter breakthrough curves were lower than the column output. Obviously, thereit was a fastbreakthrough, which bypassed the micro-lysimeters and a slowbreakthrough that was seized by the lysimeter. The similarity of the micro-lysimeter breakthroughs isexplained by thefact that all 4 micro-lysimeters liedcloseto and influenced eachother (Figs.2and5a). In columns 2 and 3 the micro-lysimeters, toagreat extent, attain higher bromidevalues earlier than the columnoutflow



1 = column output, 1/1, 1/2, 1/3 and 1/4 = micro-lysimeter

**Fig.9.** Breakthrough curves of column 1 (experimental variant 1) in units of the porevolume. C=measuredconcentration, Co=concentration of the Br pulses

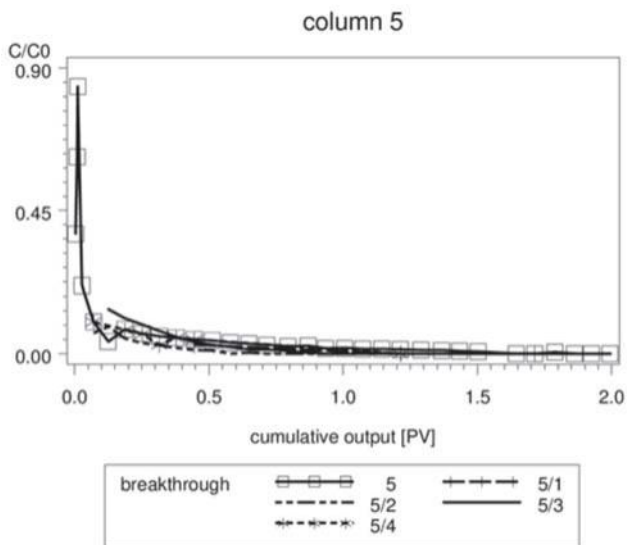


**Fig.10.** Breakthrough curves of column 5 (experimental variant 2) in units of the pore volume.  $C = \text{measured concentration}$ ,  $C_0 = \text{concentration of the Br-pulses}$

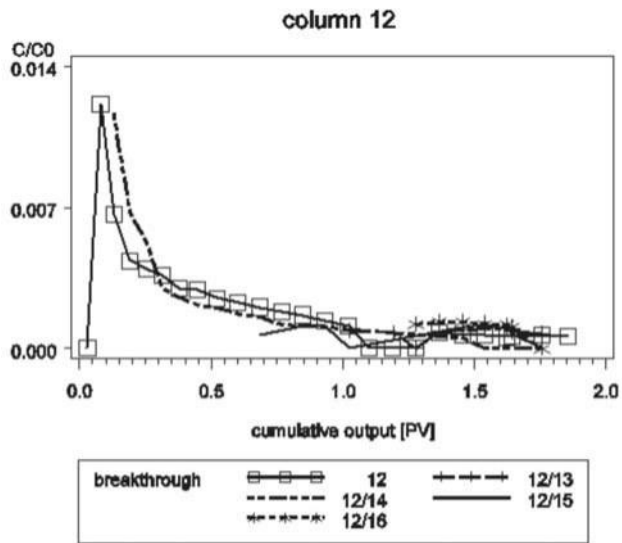


**Fig.11.** Breakthrough curves of column 12 (experimental variant 3) in units of the pore volume.  $C = \text{measured concentrations}$ ,  $C_0 = \text{concentration of the Br-pulses}$

(not shown). These lysimeters have participated in the fast breakthrough via the coarse pores, e.g. column 2 (not shown, lysimeters 5 and 7).

At least one micro-lysimeter of column 5 (Figs. 3, 6 and 10) had very clear contact to the middle of a coarse pore, which traversed through the soil column, and which possibly contributed to the fast transport. Because of the deficient initial soil contact or too low suction capacity, this lysimeter did not show the fast breakthrough. A single lysimeter of the

dry columns, lysimeter 14 of column 12 (Figs. 4, 7a and 11), showed an almost complete fast breakthrough. Of all the lysimeters of this column, this was the first to lead to soil solution leaching, and was present in the soil matrix with indirect contact to coarse porespace. This constellation, amixing of indirect contact to coarse-pore space and direct contact to the fine-pore matrix, appears to have the best pre-condition for a quick functioning of the lysimeters, above all, in dried soil substance.

#### Pore connectivity in the columns and their importance for tracer transport

For a better understanding of the total transport through the columns, the transport in topsoil and in subsoil was considered. These two were characterized by a different soil structure and pore structure. The topsoil had a more or less strongly expressed crumb structure with high porosity, whereas, the porosity in the subsoil was low, because of the clay content. Hence, its structure was strongly influenced by roots, faunal burrows, and shrinkage cracks through drying, therefore, contains macropores. Both soil regions, according to the expression of their main characteristics, differently influenced tracer transport in a column.

Luo et al. (2010) investigated quantitative relationships between macropore characteristics and two major flow and transport parameters ( $K_{\text{sat}}$  and  $\lambda$ ). Macropores played an important role. The traditional CDE modeled the BTC swell. Correlation between  $\lambda$  of the whole soil column and  $K_{\text{sat}}$  values of the B<sub>t</sub> horizon (not A) implied that the dispersivity was mainly controlled by the horizon with the lowest  $K_{\text{sat}}$  in the soil column. The most useful macropore parameters for predicting flow and transport under saturated conditions in the structured soils included macroporosity, number of paths, hydraulic radius and macropore angle. The presence of traversing pores (not necessarily macropores in the classical sense) in the subsoil influenced the velocity and concentration of the tracer transport in this part. The reconstruction of the flow pattern is difficult, although the parameters are clearly defined. This is because of the interplay of all factors, within initial and boundary conditions as water content can be different even in a small space but have a great influence. Further, the problem exists that only vertical transport mechanism was considered. As is known from dye-experiments, the horizontal transport also spreads to a good extent (Ghodratian and Jury 1990), that is why, the vertically connected pores do not lead to preferential flow.

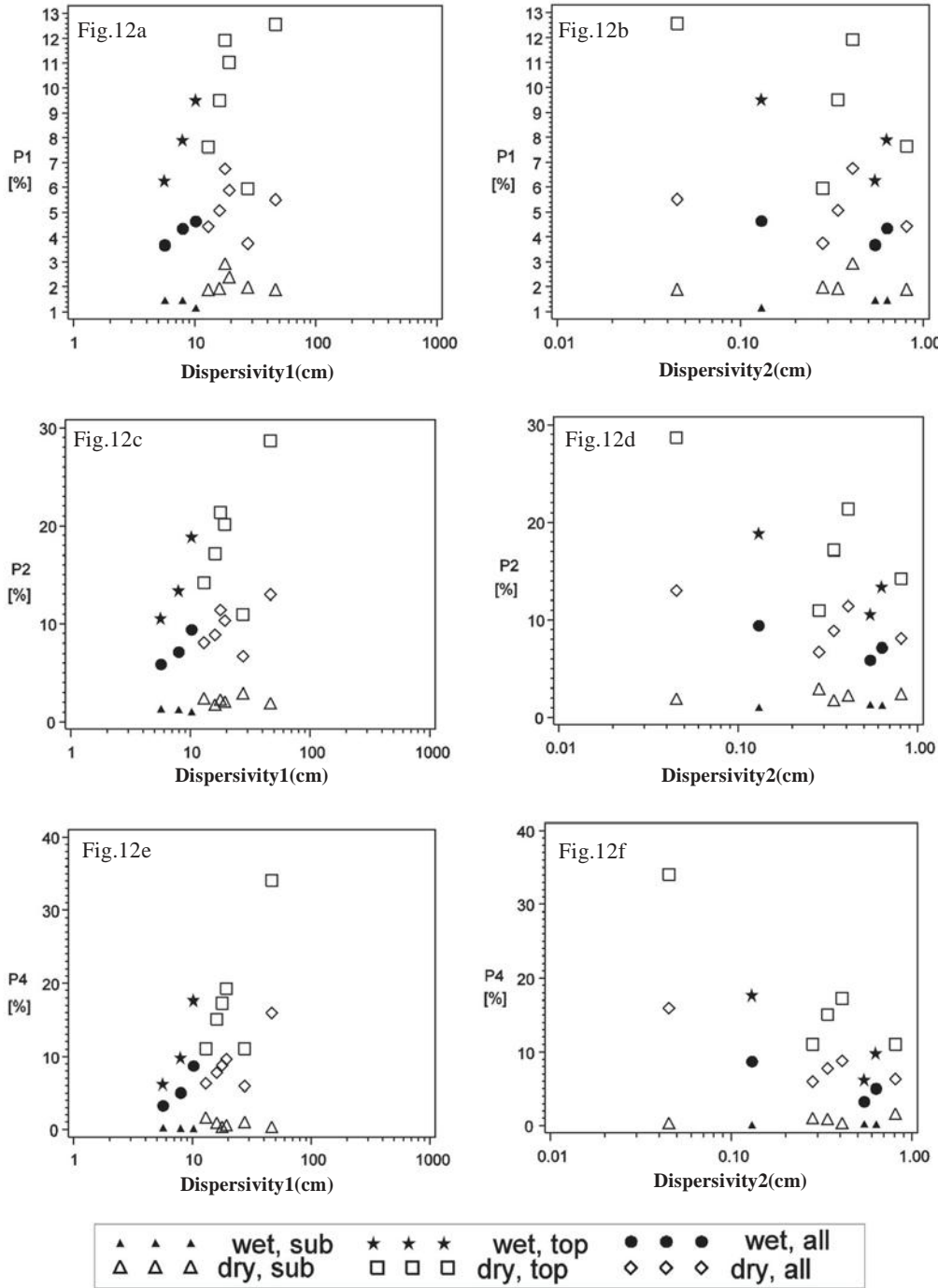


**Fig.12.** Dispersivity of the bimodal approach in relation to pore structure at three different scales (P1,P2,P4); three values for the respective column. Dispersivity1=D1/v1=fast breakthrough, dispersivity2=D2/v2=slow breakthrough (Table2). “Bottom” means subsoil of the column; “top” means topsoil and “comp.” means complete column.

In the same way, Flury *et al.* (1994) reported that a major part of the water flowed past the soil matrix. As a result, an unexpectedly small portion of the soil, possibly took part in the transport. Bootink and

Bouma (1991) observed discontinuous macropores, so-called internal catchments, which

should be integrated in water flow modeling. From studies on soil structure using x-ray CT, it was reported by Luo *et al.* (2008) that no macropores were continuous from the top to the bottom of the soil column, and some macropores became ineffective because of fair-entrainment. They concluded that

**Table 2.** Results of bimodal parameter evaluation. Retardation factor  $R = 1$ , coefficient of dispersivity ( $\text{cm}^2 \text{Day}^{-1}$ ),  $v$  = average pore water velocity ( $\text{cm Day}^{-1}$ ),  $D/v$  = dispersivity (cm),  $Br$  = Bromide quantity of the impulses (mg).

Column	$D_1/v_1$ (cm)(cm)(mg)	$D_2/v_2$	Br
1	9.0	0.18	14.3
2	8.0	0.63	16.0
3	5.7	0.54	15.0
4	14.5	0.3	15.7
5	19.3	0.0	32.4
6	38.1	0.08	34.5
8	16.0	0.34	14.3
10	24.4	0.49	16.4
11	23.1	0.26	16.8
12	12.9	0.81	11.5

macropore network by itself cannot simply be equated to a preferential flow network. Accordingly, in the description of flow process, a series of complex processes need to be considered.

In order to describe the relationship between the BTC and the soil pore characteristics, we opposed fit parameters of the CDE and soil pore indices. As explained earlier, the indexes ( $P_1, P_2$  and  $P_4$ ) were recomputed for the pore structure of a column.  $P_1$  is an index for pore structure in smaller scale. The  $P_4$  on the other hand, is an index for coarse pore structure (Fig. 1). The respective indices,  $P_1, P_2$  and  $P_4$ , are shown on the ordinate. On the abscissa, either the dispersivity of the slow ( $D_1/v_1$ ) or fast ( $D_2/v_2$ ) are shown (Fig. 12, Table 2). The symbol represents the variant of the experiment (dry, wet) and the area of the column the index applies to (top = top-soil, bottom = sub-soil, comp. = complete column).

In figures 12b, 12d and 12f, corresponding fast dispersivity values ( $D_2/v_2$ ) in relation to indexes for fine ( $P_1$ ), middle ( $P_2$ ), or coarse ( $P_4$ ) pores were presented. At all three scales these figures showed a negative relationship to dispersivity, which increased with decreasing air content. This relationship was stronger for coarse pore indexes in topsoil. The transport pathway appeared to be shortened by higher air content, which lowered fast dispersivity. When coarse pores were present in the columns ( $P_4$ ), then with fast breakthrough, uniform flow was to be expected, without the heterogeneity of pathway of water and chemical movement. Nearly linearly decreasing lines could be observed (Fig. 12f) for topsoil and whole column indexes. This happened to a lesser extent even with more finely divided porespace

(Fig. 12d). The slow dispersivity values had a positive relationship to the pore indices for all scales (Fig. 12a, 12c and 12e) and soil areas, which was nearly linear in all scales. With growing pore content the heterogeneity of the pathways increased. Again, this relationship was more apparent in topsoil.

All results have to be considered with a bit of caution, as the CDE fit was using a model, which for the dry columns might be questionable. As a mathematical model it reached plausible dispersivity values, though. It explains why we could not detect differences among the soil columns just by visualizing. It can be assumed that all columns showed macropore transport, which was not linked to dispersivity of the sub-soils.

## Conclusions

The 3D reconstruction of the porous system can be used to discuss the suction performance of individual micro-lysimeters and for explaining the breakthrough curves of micro-lysimeters. A numeric pore index representing a volume's pore content at a specific scale can be computed from CT data, and does have a relation to flow parameters. The pore index has generally a negative linear relationship with the fast dispersivity, and a positive linear relationship with the slow dispersivity. These relations suggest that with increasing porosity, the heterogeneity of the pathways increases. We conclude that the CT images like cross-sections and 3D reconstructions provide an interesting and quite unique insight into the soil poresystem after moderate drying. Cross-sections visualizing the pore contact of micro-lysimeters' tips may help to interpret soil water monitoring in a better way.

## References

- Beckmann, T., Kücke, M., Hasenpusch, K. and Altemüller, H.J. (1992) Einbaubedingte Gefügeänderungen in der Bodenzone um keramische Saugkerzen. *Zeitschrift für Pflanzenernährung und Bodenkunde* **155**, 247-250.
- Booltink, H.W.G. and Bouma, J. (1991) Physical and morphological characterization of by-passflow in a well-structured clay soil. *Soil Science Society of America Journal* **55**, 1249-1254.

- Bouma,J.andWosten,J.H.M.(1979)Flowpatternsduring extendedunsaturatedflowintwo,undisturbed swellingclaysoilwithdifferentmicrostructures.*Soil ScienceSocietyofAmericaJournal***43**,16-22.
- Borges,J.A.R.andPires,L.F.(2012)Representative elementaryareainsoilbulkdensitymeasurementsthrough gammaraycomputedtomography.*Soiland TillageResearch***123**,43-49.
- Flury,M.,Fluehler,H.,Jury,W.A.andLeuenberger,J. (1994)Susceptibilityofsoiltopreferentialflowof water:Afieldstudy.*WaterResourcesResearch***30**, 1945-1954.
- Gantzer,C.J.andAnderson,S.H.(2002)Computed tomographicmeasurementofmacroporosityinchisel-diskandnon-tillageseedbeds.*SoilandTillage Research***64**,101-111.
- Ghodrati,M.andJury,W.A.(1990)Afieldstudyusing dyestocharacterizepreferentialflowofwater.*Soil ScienceSocietyofAmericaJournal***54**,1558-1563.
- Grevers,M.C.J.,DeJong,E.andArnaud,R.J.St(1989) ThecharacterizationofsoilmacroporositywithCT scanning.*CanadianJournalofSoilScience***69**,629-6.
- Hainsworth,J.M.andAylmore,L.A.G(1983)Theuseof computer-assistedtomographytodeterminespatialdistributionofsoilwatercontent.*AustralianJournal ofSoilResearch***21**,435-443.
- Heijs,A.W.J.,Lange,J.,deSchoute,J.F.andBouma,J. (1995)Computedtomographyasatoolfordestructiveanalysisofflowpatternsinmacroporousclays oils.*Geoderma***64**,183-196.
- Heijs,A.W.J.,Ritsema,C.J.andDekkar,L.W.(1996)Three dimensionalvisualizationofpreferentialflowpattern intwosoils.*Geoderma***70**,101-116.
- Kumar,S.,Anderson,S.H.andUdawatta,R.P.(2010) Agroforestryandgrassbufferinfluenceon macroporesmeasuredbycomputedtomographyunder grazedpasturesystems.*Soil ScienceSocietyof AmericaJournal***74**,203-212.
- Luo,L.F.,Lin,H.S.andHalleck,P.(2008)Quantifying soilstructureandpreferentialflowinintactsoilusing X-raycomputedtomography.*Soil ScienceSocietyof AmericaJournal***72**,1058-1069.
- Luo,L.F.,Lin,H.S.andSchmidt,J.(2010)Quantitative relationshipbetweensoilmacroporecharacteristicsand preferentialflowandtransport.*Soil Science Societyof AmericaJournal***74**,1929-1937.
- Nielsen,D.R.andBiggar,J.W.(1962)Miscible displacement.3.Theoreticalconsiderations.*Soil ScienceSocietyof AmericaProceedings***26**,216-221.
- Peyton,R.L.,Haefner,B.A.,Anderson,S.H.andGantzer, C.J.(1992)ApplyingX-rayCTtomeasuremacropore diametersinundisturbedsoilcores.*Geoderma***53**, 329-340.
- Petrovic,A.M.,Siebert,J.E.andRieke,P.E.(1982)Soil bulkdensityanalysisinthreedimensionsbycomputer tomographicscanning.*Soil ScienceSocietyof AmericaJournal***46**,445-450.
- Pierret,A.,Capowiez,Y.,Belzunces,L.andMoran,C.J. (2002)3Dreconstructionandquantificationof macroporesusingX-raycomputedtomographyand imageanalysis.*Geoderma***106**,247-271.
- Spangenberg,A.,Cecchini,G.andLamersdorf,N.(1997) Analysingtheperformanceofamicrosolsolutionsampling deviceinalaboratoryexaminationanda fieldexperiment.*PlantandSoil***196**,59-70.
- Spangenberg,A.,Nagarajarao,Y.andHinz,Ch.(2011) Descriptionoftracertransportthroughmoistanddried soilcolumnsusingabimodalCDEapproach. *FreseniusEnvironmentalBulletin***20**,616-622.
- Taina,L.A.,Heck,R.J.andElliot,T.R.(2008)Application ofX-raycomputedtomographytooilscience:A literaturereview.*CanadianJournalofSoilScience* **88**,1-20.
- Toride,N.,Leij,F.J.andvanGenuchten,M.Th.(1995)The CXTFITcodeforestimatingtransportparametersfromlaboratoryorfieldtracerexperiments.U.S. SalinityLaboratory,U.S. DepartmentofAgriculture, Riverside, CaliforniaResearchReport,137.
- vanGenuchten,M.Th.andAlves,J.W.(1982)Analytical solutionsontheone-dimensionalconvective-dispersive solutetransportequation.*USDepartmentof AgricultureTechnicalBulletin*,133-192.
- Warner,J.S.,Nieber,J.L.,Moore,I.D.andGeese,R.A. (1989)Characterizingmacroporesinsoilby computed tomography.*Soil ScienceSocietyof AmericaJournal* **53**,653-660.